# Anomalous behavior of water around sodium dodecyl sulphate micelles

Shubhra Ghosh Dastidar and Chaitali Mukhopadhyay*
*Department of Chemistry, University of Calcutta, 92. A.P.C. Road, Kolkata 700 009, India*
(Received 26 July 2004; published 1 December 2004)

The dynamics, structural properties, and energetics of hydration water around a sodium dodecyl sulphate micelle have been investigated using molecular dynamics simulation. A clear revelation of the slow dynamics of the hydration water has been made by separate measurements of the rotational and translational properties. Calculated diffusion coefficients fall within the range of experimentally observed quantities. The water-micelle head group (MHG) hydrogen bond is more stable (by an amount ~7.0 kcal/mol) compared to the water-water hydrogen bond. The difference in stability of the water monomers forming different numbers of hydrogen bonds ($n=0,1,2$) with the MHG has clearly been shown from the analyses of their rotational relaxation, residence times, as well as the energy of interaction with different components of the system. The singly hydrogen-bonded water species is the most abundant and stable. The entropy plays the key role in controlling the relative abundance of the different species.

DOI: 10.1103/PhysRevE.70.061901 PACS number(s): 87.15.−v, 66.10.−x

## I. INTRODUCTION

The altered structure and dynamics of water molecules at the interfaces of biological macromolecules and other self-organized assemblies have received great attention recently [1,2]. Experiments [1,3–9] performed extensively during the last decade have shown that the dynamics of hydration water ("biological water") is slower than that of bulk water. Atomistic simulations are revealing very interesting details of the structure, energetics, and dynamics of water molecules near surfaces of proteins [2,10], DNA [11], lipid bilayers [12], etc., and almost all reports have indicated a slowing down of water molecules near the interface. There are reports that hydration water is crucial for the functionality of biological macromolecules [13–16]. At the membrane surface the interaction with interfacial water constitutes the initial events that take place during many biological recognition, insertion, and transport processes. The complexity of membrane interfaces makes them less amenable to experiments. Micelles, on the other hand, provide a relatively simple mimic of a membrane and are being extensively used to study a variety of peptide-membrane interactions [17,18]. The nature of hydration water at the micellar interface has attracted some attention in recent years. In a series of reports [19–22] on cesium pentadecafluorooctanate (CsPFO) micellar systems, interfacial water molecules have been classified into three categories: the first two are either singly or doubly hydrogen bonded (H bond) to the polar micellar head groups (MHG's) and the third category included water molecules that are not H bonded to MHG's. The bound water molecules are stabilized [22] by an energy of ~2.0–4.0 kcal/mol. It was suggested that entropy is a key factor in determining the relative abundance of the individual species. The dramatically slow dynamics of interfacial water has been attributed to the long-lived hydrogen bonds between water and surfactant head groups [20,21].

Sodium dodecyl sulphate (SDS) micelles having a more complicated head group structure ($SO_4^-$ as compared to $COO^-$ in CsPFO) are extensively used to study membrane-peptide interactions. Earlier computer simulation reports by Bruce *et al.* [23] on the water environment near SDS micelle focused on the structural and dynamical aspects including the relevant radial distribution functions. It has been revealed there that the water molecules do not penetrate the hydrocarbon core and the hydrogen-bond network of solvent molecules is disturbed by the hydrogen bond between water and head group atoms. They have also indicated that the rotational movement is more affected than translational in the first hydration shell [23]. However, statistics on different water species are not extensive and a more detailed investigation about the nature of the different types of hydration water including their relative abundance, rotational and translational diffusions, residence times, and stabilization energies seems worthwhile.

We report here the quantitative measurements of the dynamical properties and the detailed analysis of the water structure in the first hydration layer of SDS micelle including their identity, binding properties, and thermodynamics involved. The simulation strategy as well as the force field adapted in this case is different from previous studies. Usually in order to cut down the computational time such simulations are run after freezing the vibration of bonds and thereby increasing the integration time step to 2 fs [23]. However, freezing of bonds containing hydrogens may adversely affect the calculated dynamics of the hydrogen bonds as it has been shown that bond vibrations can influence the lifetime of the hydrogen bonds [24]. In the present work no constraint on the vibrations of the bonds has been applied and a shorter integration time step of 1 fs has been taken. Our simulation is in agreement with those reported [19–22] for CsPFO in identifying the different types of water monomers present in the first hydration layer. This distinction in water monomers has been found to be appropriate also from calculation of their stabilization energy. The diffusion coefficients calculated for water molecules in various hydration shells match quite well with the experimental data. The resi-

*Corresponding author. FAX: 91-33-2351-9755.

 

dence times of water in the first and subsequent hydration layers demonstrated clearly the presence of fast and slow components. The structure and dynamics of the singly- and doubly-hydrogen-bonded species have been categorized.

## II. SIMULATION DETAILS

The structure of a SDS monomer was generated using the CHARMM (Chemistry at Harvard Macromolecular Mechanics) package (version No. 28b1). Copies of the monomer were rotated and translated properly to construct an almost spherical micelle of radius ~21 Å containing a cavity of radius ~3.5 Å at the center. The micelle was consisting of 62 monomers. The aggregation number of SDS has been reported to be in the range 60–70 at room temperature [25,26], and our choice of 62 monomers was arbitrary within the specified range. The micelle was minimized in vacuum and then was placed in a cubic water box of side length 60 Å containing 8000 TIP3P water molecules (which corresponds to a density ~1 $g/cm^3$). The water molecules residing within the 10 Å distance from the center of the micelle were deleted [27], and then any other water molecules whose oxygen atom resides within 2.6 Å distance from any heavy atom of the micelle were deleted. Sixty-two sodium ions were added to the system by replacing the water molecules randomly to maintain the overall electroneutrality of the system. The resulting system contained 62 SDS monomers, 6756 water molecules, 62 sodium counter-ions, and overall 22 934 atoms. The system was then energy minimized, heated to 300 K, and equilibrated. After that the resulting box size was 61 Å×61 Å×61 Å. A 2.8-ns-long *N-V-T* simulation was carried out with 1 fs integration time step, CHARMM force field, and parameter of version 27. A 12-Å cutoff for nonbonded interactions was used, and the nonbonded lists were updated after every 25 fs. Long-range electrostatic and van der Waals interactions were taken into account using a shifting function. A periodic boundary condition was applied to the system to minimize the edge effect. Different types of analyses need different types of sampling intervals and trajectory lengths. Coordinates were usually saved after each 250 fs, and in addition to that the snapshots during the last 30 ps of the whole trajectory were saved after each 15 fs, which gave a resolution sufficient to study the short time dynamics [28]. The diffusion properties were analyzed with this trajectory of 15 fs resolution. We have not considered the first 1 ns of the total 2.8 ns trajectory (TRAJ1) for the analysis so that the system equilibrates sufficiently before the analysis starts. Different portions of the last 1.8 ns of the trajectory have been used for the analysis. A cubic water box of 32 Å side length containing only 1000 water molecules was simulated with similar protocol, and this trajectory has been used to generate the data for "bulk" water which is the system of reference. This trajectory has been referred as TBLKC. The data presented in this work have been extracted from these two trajectories.

In this article we have discussed the justification of using a spherical cutoff for long-range electrostatics. We have extended the TRAJ1 for another 0.5 ns using the particle mesh Ewald (PME) summation method, and this extension has been referred as TRAJ2. The bulk water was also simulated using PME (referred as TBLKP) in addition to the trajectory "TBLKC" run with the cutoff method. The diffusion properties of water obtained from the different methods of simulation have been compared. We have performed the simulation on a PIII IBM server at our department. MICROCAL ORIGIN 5.0 has been used for plotting the data, drawing the figures, and for giving different types of fits (e.g., stretched exponential decay) to the data.

## III. RESULTS

In this study the focus was on the properties of the solvents. The solvent model and the simulation scheme were chosen in such a way that the bulk properties of the solvent— i.e., water—could be produced close to the experiments. It was highly nontrivial to choose the method of tackling the long-range electrostatic interactions. Though the Ewald summation technique is more accurate than ordinary cutoff methods, it has been shown that the TIP3P model for water gives better data (i.e., closer to the experiments) when it is treated with a cutoff method coupled with shifting functions for nonbonded interactions rather than using the Ewald summation technique [29,30]. Makarov *et al.* [30] clearly reported the overestimation of the water diffusion with the Ewald technique. Several reports [29–35] on the self-diffusion coefficients of TIP3P water indicate that the choice of method for handling the long-range interactions, nonbonding cutoff distances, introduction of shifting potential function in case of cutoff methods dramatically change the observable properties. Using these different strategies the reported [29–35] self-diffusion coefficient of water ranges between $2.3\times10^{-5}$ and $7.0\times10^{-5}$ $cm^2/sec$ for the original and modified TIP3P models. In some reports [29,30] it has been shown that the use of the Ewald summation technique yields an elevated diffusion coefficient ($\sim5\times10^{-5}$ $cm^2/sec$), whereas with a 12-Å nonbonding cutoff the calculated water properties are closer to the experiments. In our case, the self diffusion coefficient of "bulk" water obtained from the PME trajectory (TBLKP) is $3.8\times10^{-5}$ $cm^2/sec$ (see Table I) whereas using a 12-Å cutoff and shifted potentials (TBLKC) yielded a value $2.8\times10^{-5}$ $cm^2/sec$, which is closer to the experiments ($2.3\times10^{-5}$ $cm^2/sec$) [36]. It has been suggested by Alper *et al.* [37] that for solvent properties the use of the Ewald summation technique should yield poor results since the TIP3P model was originally optimized with cutoff methods. Our results indicate that the present simulation procedure produces the diffusion properties for the micellar system and the "bulk" water from the trajectories TRAJ1 and TBLKC, respectively, much closer to the experiments than the previous reports [23] ($D=5.3\times10^{-5}$ $cm^2/sec$) on a similar system.

### A. Radial distributions of water

Various types of properties reported in this article which are averaged over water shells (e.g., $R=1-4$ Å, $R=5-8$ Å, etc.) acknowledged only those water molecules, which do not leave that specified water shell within the time interval of

TABLE I. Diffusion coefficient ($D$) values for water in different layers around micelle head groups obtained from the simulation using spherical cutoff and shifted potential (VSHIF), which has been compared with the $D$ values obtained from the simulation of the same system using PME technique. The $D$ values for bulk water for each method of simulation and experiment [36] have been given.

| $R$(Å) | $D(10^{-5}$ cm$^2$/sec) | $D(10^{-5}$ cm$^2$/sec) | $D(10^{-5}$ cm$^2$/sec) (experimental) [36] |
|---|---|---|---|
| 1–4 | 1.7[a] | 3.0[b] | |
| 5–8 | 2.3[a] | | |
| 9–12 | 2.6[a] | 3.7[b] | |
| | | | 1.3 (278 K) |
| Bulk water | 2.8 | 3.8 | 1.8 (288 K) |
| | (TBLKC) | (TBLKP) | 2.3 (298 K) |

[a]Using a spherical cutoff coupled with a shifted potential (TRAJ1).
[b]Using PME (TRAJ2).

the calculation. $R$ defines the water shells, and $R$ is measured from the micelle head group oxygen (MHGO). As a starting point we need to have information about the distribution of water molecules around the micellar head groups since it is impossible otherwise to define a cutoff distance for the first layer of hydration. Calculation of a radial distribution function is very useful to get a picture about the distribution [2]. The radial distribution function $g(r)$ is calculated as follows:

$$g_\alpha(r) = \frac{\langle \Delta N_\alpha(r) \rangle}{4\pi N_w \rho \Delta r}, \tag{1}$$

where $\langle \Delta N_\alpha(r) \rangle$ is the number of water molecules averaged over time, within a distance $r \pm \Delta r/2$ from a hydration site $\alpha$, $\rho$ is the density of the bulk water, and $N_w$ is the total number of water molecules in the system. $\Delta r$ was chosen as 0.1 Å.

In Fig. 1 the plot of the O-O radial distribution—i.e., the MHG oxygen atoms (MHGO) versus water oxygen atoms—shows that there is a concourse of water molecules at a distance 2.7 Å. This peak arises due to the micelle-water hydrogen bonding. We have used a value of 4 Å as a cutoff distance for defining the first layer of hydration, and this distance is measured from the MHGO atoms. Use of this value ensures the inclusion in the first layer of almost all water molecules that have a chance to form H bonds with the MHGO. To compare the properties averaged over the water layers of similar thickness we choose the first water layer of $R=1-4$ Å rather than $R=0-3$ Å and take the subsequent layers at $R=5-8$ Å and $R=9-12$ Å. The layer for $R=0-1$ Å was ignored to avoid the void region on the micelle surface which has been observed from Fig. 1.

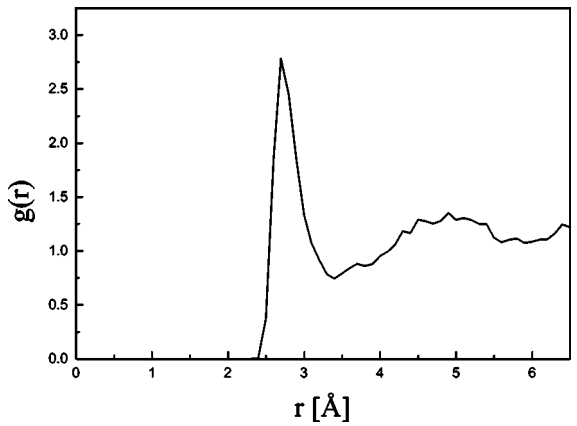


FIG. 1. Micelle-water radial distribution around SDS micelle as a function of the distance between water oxygen and the nearest micelle head group oxygen atom.

### B. Categorization of MHG-water hydrogen-bonded species

The water monomers in the first hydration layer can exist as H bonded (labeled as "bound water") to the MHG oxygen atom or as free—i.e., having no H bond with the MHG. In SDS micelle MHGO's can only act as acceptor. The criteria for the H bond was set such that the OHO cutoff angle was 120° and a maximum value of 2.4 Å for the O-H length was allowed. These cutoff values were compatible with the CHARMM force field [38]. The water monomers which form a single H bond and a double H bond with the MHG have been labeled as 1HBW and 2HBW, respectively, and the water molecules residing in the first hydration layer having no H bonds with the MHG have been labeled as FRW—i.e., free water.

### C. Rotational diffusion

The information about the influence of the interaction between the macromolecules or molecular assemblies and the solvent on the diffusive properties of hydration water can be obtained from the study of the rotational diffusion of the water electrical dipole. The reorientational dynamics of the water electrical dipole $\vec{\mu}_i$ can be analyzed by means of the autocorrelation function $\Gamma_1$ defined as [39–41]

$$\Gamma_1(t) = \langle P_1[\vec{\mu}_i(0) \cdot \vec{\mu}_i(t)] \rangle, \tag{2}$$

where $P_1$ is the $l$th-order Legendre polynomial and $\vec{\mu}_i(t)$ is the unit vector along the dipole axis of the $i$th water molecule at time $t$; the bracket "$\langle\rangle$" indicates both the average over solvent molecules and different time origin. The first- and second-order (i.e., $l=1$, $l=2$) Legendre polynomials are usually investigated. Here we report for the second-order function. The relaxation of rotational correlation function of the hydration water can be fitted with a sum of two stretched exponential functions [2]:

$$\Gamma_2(t) = Ae^{-(t/\tau_s)^{\beta_s}} + Be^{-(t/\tau_l)^{\beta_l}}, \tag{3}$$

where the $l$ and $s$ suffixes stand for the longer and shorter components of the relaxation orientation time $\tau$. $\beta$ is the stretching parameter and is a measure of the deviation from the exponential character of the decay. This type of time behavior is termed Kohlrausch-Williams-Watts (KWW) relaxation [42,43]. The $A$ and $B$ values tell the relative contribution from the shorter and longer components of the decay, respectively. Figure 2 and Table II show that the relaxation becomes fast as we go away from the MHG, and this is

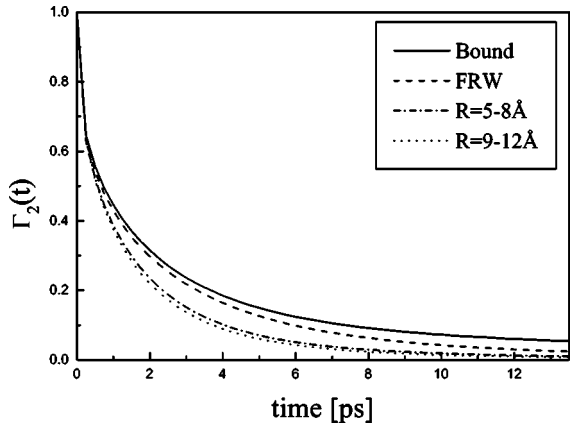


FIG. 2. Rotational relaxation of the water molecules at various shells of water around SDS micelle: bound (solid line) in the first layer, free or FRW (dashed line) in the first layer, $R=5-8$ Å (dash-dotted line) and $R=9-12$ Å (dotted line). Fitting parameters have been given in Table II.

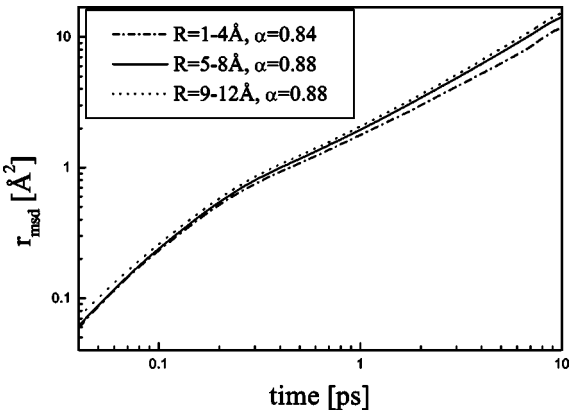


FIG. 3. Log-log plot of the mean-square displacement ($r_{\mathrm{msd}}$) of water molecules (extracted from TRAJ1) at various shells around SDS micelle: $R=1-4$ Å (dash-dotted line), $R=5-8$ Å (solid line), and $R=9-12$ Å (dotted line). The $\alpha$ values reported in the figure have been calculated by a linear fit of the data of last 8 ps of a total 10 ps duration of the calculation.

indicated by the decreasing values of decay constants as the distance from the MHG increases. We have identified the water monomers, which are either bound (1HBW and 2HBW) or free (FRW) at the start of the calculations in the first layer, and the difference in their rotational dynamics has been shown in the table and figure mentioned above.

### D. Diffusion properties of the water molecules

Solvent mobility is most conveniently described by the diffusion coefficient $D$ related to the slope of the molecular mean-square displacements (MSD) by the Einstein relationship, which in $d$ dimension has the following form [44]:

$$D = \frac{1}{2d} \lim_{\Delta t \to \infty} \frac{\langle |\vec{r}_i(t) - \vec{r}_i(0)|^2 \rangle}{\Delta t} = \frac{1}{2d} \lim_{\Delta t \to \infty} \frac{\langle \Delta r^2 \rangle}{\Delta t}, \qquad (4)$$

where $\vec{r}_i(t)$ and $\vec{r}_i(0)$ are the position vectors of the $i$th solvent molecule at time $t$ and at time $t=0$ respectively. The numerator $\langle |\vec{r}_i(t) - \vec{r}_i(0)|^2 \rangle$ represents the MSD of the position vectors which is referred to as $r_{\mathrm{msd}}$ in Fig. 3. The "$\langle\rangle$" sign indicates the averaging over both the time origin and the solvent molecules. This method of calculation of $D$ requires the storing of the coordinates with a higher frequency (here we have used 15-fs intervals) during the simulation run [45]. The diffusion coefficients for the water at different layers has been calculated (Table I) from the slope of the linear fit of the plot (Fig. 3) of $r_{\mathrm{msd}}$ of water oxygen atoms versus time of last 8 ps duration of a total 10 ps trajectory length analysis with a resolution of 15 fs (the $\Delta t$ being 8 ps). The values of $R$ define the water layer on which the individual calculations have been made. The diffusion coefficient ($1.7 \times 10^{-5}$ cm$^2$/sec) for water molecules in the layer $R=1-4$ Å indicates the least tendency to diffuse, whereas for $R=9-12$ Å we got $D=2.6\times10^{-5}$ cm$^2$/sec. The water in the first hydration layer is 1.6 times less diffusive than the "bulk" water whose diffusion coefficient is $2.8 \times 10^{-5}$ cm$^2$/sec. Table I also contains $D$ values obtained from the experiments [36] at various temperatures. The $D$ values obtained for the run with the PME method (TRAJ2) have been shown in Table I for a comparison.

TABLE II. Fitting parameters for the data obtained for rotational relaxation calculated according to Eqs. (2) and (3) for water molecules residing at various shells of water around micelle. Bound water and FRW both resides in the shell $R=1-4$ Å. Data for bulk water have also been given for comparison.

| $R$ (Å) | $A$ | $\tau_s$ (ps) | $\beta_s$ | B | $\tau_1$ (ps) | $\beta_1$ |
|---|---|---|---|---|---|---|
| Bound | 0.62 | 0.84 | 0.33 | 0.38 | 2.20 | 0.90 |
| FRW | 0.53 | 0.60 | 0.33 | 0.45 | 2.09 | 0.90 |
| 5–8 | 0.51 | 0.36 | 0.38 | 0.49 | 1.76 | 0.91 |
| 9–12 | 0.49 | 0.37 | 0.40 | 0.51 | 1.62 | 0.90 |
| Bulk(TBLKC) | 0.49 | 0.37 | 0.40 | 0.51 | 1.67 | 0.90 |

Instead of a linear change in the MSD value of water with time calculated from the Einstein equation a time-dependent change of the slope of the plot $r_{\mathrm{msd}}$ versus time has been observed which is indicative of the anomalous diffusion at the micelle-water interface that has been previously observed at the protein water interface [2,10,46]. Due to the presence of anomalous diffusion, the MSD follow the law

$$\langle \Delta r^2 \rangle \sim t^{\alpha}. \qquad (5)$$

The log-log plot (Fig. 3) of $r_{\mathrm{msd}}$ versus time is helpful to get the values of $\alpha$. The abrupt change of the slope indicates the establishment of the diffusive regime after ballistic regime that lasted for the first 0.2 ps. Before the diffusive regime was established, the initial slope for the all layers of water gave $\alpha \sim 2$, which became less than 1 when the diffusive regime was established and did show a distinct and lowest value (see Fig. 3) of $\alpha$ for the shell $R=1-4$ Å($\alpha=0.84$). The water at the larger distance did show almost similar values of $\alpha=0.88$ within the time interval of the calculation.

### E. Residence time analysis

To understand the translational diffusive property of the layers more clearly, calculation of the water residence times

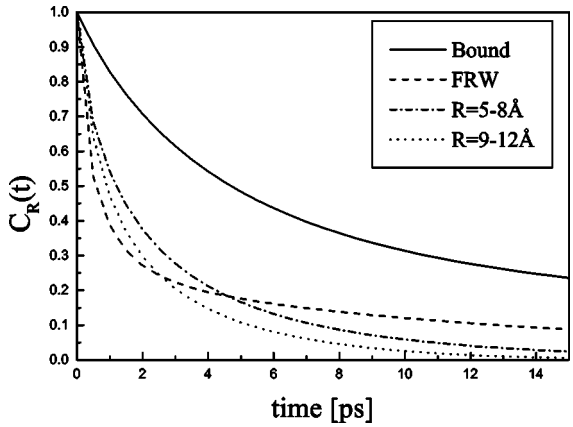


FIG. 4. Decay of survival time correlation function of water at various shells of water around SDS micelle: bound (solid line) in the first layer, free or FRW (dashed line) in the first layer, $R=5-8$ Å (dash-dotted line), and $R=9-12$ Å (dotted line). Fitting parameters have been given in Table III.

is essential. Water residence times can provide useful insights into the structural and translational dynamical behavior of interfacial water in the first or successive hydration shells of the macromolecular atoms exposed to the solvent [2]. Commonly, the residence time is evaluated from a survival time correlation function $C_R(t)$, describing the relaxation of the hydration shells of a macromolecule or molecular assemblies [2]. The "layer survival time correlation function" can be defined as

$$C_R(t) = \frac{1}{N_w} \sum_{j=1}^{N_w} \frac{\langle P_{R,j}(0) P_{R,j}(t) \rangle}{\langle P_{R,j}(0)^2 \rangle}, \tag{6}$$

where the $P_{R,j}$ is a binary function that takes a value of 1 if the $j$th water molecule stays in the layer of thickness $R$ for a time $t$ without getting out in the interim of this interval and of zero otherwise. This quantity $C_R(t)$ measures the probability that a water molecule remains in a given layer for a time $t$. The relaxation trend of the $C_R(t)$ provides information about the local dynamics of the hydration waters. A sum of three exponential functions was fitted to the data according to the following equation:

$$C_R(t) = A_1 e^{-(t/\tau_1)} + A_2 e^{-(t/\tau_2)} + A_3 e^{-(t/\tau_3)}. \tag{7}$$

The decay for the various water layers is shown in Fig. 4 and the values of the decay constants have been given in Table III. The $A$, $B$, and $C$ values indicate the relative contribution from the different time scale motions to the decay. We have separately reported the decay of survival time correlation function for bound and free water rather than averaging it over all the waters in the first layer. Figure 4 and Table III show that bound water resides for the longest in a particular water layer among all the water molecules in the system.

### F. Lifetime of the water monomers in the first layer

The bound water in the first layer can be identified either as 1HBW or as 2HBW at any instance. Since they are always in dynamic equilibrium with the other species, during the course of the simulation they can leave the first hydration layer or be converted to FRW. A similar kind of conversion was also true for FRW; it has always the chance to be converted to either "bound" or "bulk." So we have also investigated the lifetime of different water species in the first layer. A function $C_W$ has been defined for this calculation [21]:

$$C_W(t) = \frac{\langle h(0) h(t) \rangle}{\langle h \rangle}, \tag{8}$$

where $h(t)$ is 1 if a water monomer preserves its identity at time $t$ and otherwise zero; i.e., if a 1HBW selected at $t=0$ remains as 1HBW at $t$ then $h(t)$ will be taken as 1, but otherwise zero. $C_W$ allows the reformation of bonds that are broken at some intermediates. Figure 5 shows that the decay

TABLE III. Fitting parameters for the data obtained for the decay of survival time correlation function calculated according to Eqs. (6) and (7) for water molecules residing at various shells of water of similar thickness around micelle.

| | | |
|---|---|---|
| Bound | $A_1=0.02$ | $\tau_1=0.50$ ps |
| | $A_2=0.59$ | $\tau_2=3.74$ ps |
| | $A_3=0.39$ | $\tau_3=27.40$ ps |
| FRW | $A_1=0.60$ | $\tau_1=0.41$ ps |
| | $A_2=0.22$ | $\tau_2=2.75$ ps |
| | $A_3=0.18$ | $\tau_3=22.68$ ps |
| $R=5-8$ | $A_1=0.22$ | $\tau_1=0.29$ ps |
| | $A_2=0.44$ | $\tau_2=1.74$ ps |
| | $A_3=0.34$ | $\tau_3=5.60$ ps |
| $R=9-12$ | $A_1=0.18$ | $\tau_1=0.27$ ps |
| | $A_2=0.37$ | $\tau_2=0.94$ ps |
| | $A_3=0.45$ | $\tau_3=3.46$ ps |

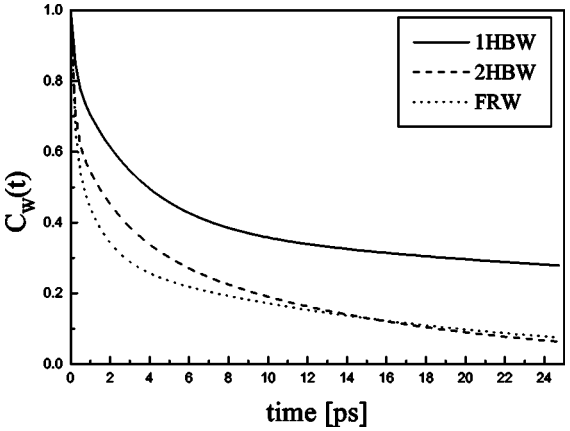


FIG. 5. Decay of the $C_w$ function [see Eq. (8)] for different water species in the first hydration layer showing the lifetime of those species: 1HBW (solid line), 2HBW (dashed line), and FRW (dotted line). Fitting parameters [see Eq. (9)] have been given in Table IV.

TABLE IV. Fitting parameters for decay of the lifetime correlation function ($C_w$) of various water species in the first hydration layer calculated according to Eqs. (8) and (9). The $\tau$ values give the lifetime of the 1HBW, 2HBW, and FRW.

| | | |
|---|---|---|
| 1HBW | $A_1=0.18$ | $\tau_1=0.23$ ps |
| | $A_2=0.44$ | $\tau_2=3.38$ ps |
| | $A_3=0.38$ | $\tau_3=79.00$ ps |
| 2HBW | $A_1=0.33$ | $\tau_1=0.17$ ps |
| | $A_2=0.28$ | $\tau_2=2.26$ ps |
| | $A_3=0.39$ | $\tau_3=13.60$ ps |
| FRW | $A_1=0.37$ | $\tau_1=0.17$ ps |
| | $A_2=0.33$ | $\tau_2=1.40$ ps |
| | $A_3=0.30$ | $\tau_3=17.80$ ps |

of $C_W$ is slowest for the 1HBW. A fit of a sum of three exponentials [20,21] for $C_W$ has been able to clearly show the wide variation of the decay constants:

$$C_W(t) = A_1 e^{-(t/\tau_1)} + A_2 e^{-(t/\tau_2)} + A_3 e^{-(t/\tau_3)}. \quad (9)$$

The fitted data have been shown in Table IV. The dynamical stability of 1HBW species over the 2HBW or FRW is evident from the $\tau$ values. The low contribution ($A_1=18\%$) from the fast component ($\tau_3=0.23$ ps) and the higher contribution ($A_3=38\%$) from a very slow component ($\tau_3=79.0$ ps) of the decay have been observed for 1HBW species.

### G. Solute-solvent interactions at the first hydration layer

The preference of the water monomers to form a H bond with a MHG rather than with another water molecule could be analyzed in terms of water-micelle interaction energies.

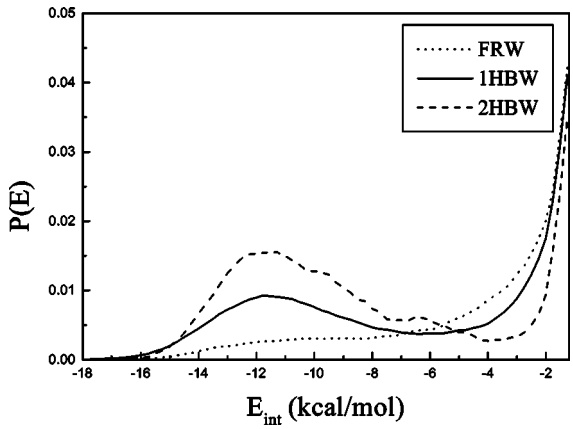


FIG. 6. Potential energy distributions for pairs of molecules of the type 1HBW-MHG (solid line), 2HBW-MHG (dashed line), and FRW-MHG (dotted line).

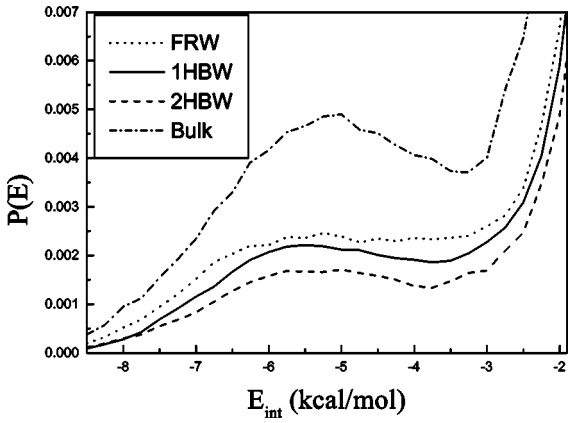


FIG. 7. Potential energy distributions for pairs of molecules of the type 1HBW-water (solid line), 2HBW-water (dashed line), and FRW-water (dotted line). The dash-dotted line for the bulk denotes the pair-interaction energy distribution of the water molecules in pure water obtained from TBLKC trajectory.

Two types of pair energy distributions, MHG-water (Fig. 6) and water-water (Fig. 7), have been calculated. Figures 6 and 7 show the probability $P(E)$ as a function of interaction energy $E_{\text{int}}$ (in kcal/mol). For the MHG-water interaction Fig. 6 shows a peak roughly around −12 kcal/mol and the relative height of the peaks for the different water species makes it clear that 2HBW gets maximum stability from this interaction and the FRW species do not have much benefit, whereas 1HBW is an intermediate between these two. The peak around −12 kcal/mol is indicative of MHG-water H-bond formation. In Fig. 7 the water-water pair energy distribution shows a slight peak around −5.0 kcal/mol for "bulk" water arising plausibly due to the water-water H bond [22] and the decrease in height of the peak in the order bulk $\gg$FRW$>$1HBW$>$2HBW is due to the decrease in probability of water-water H-bond formation in the same order. In Fig. 8 total interaction energy of a water monomer with

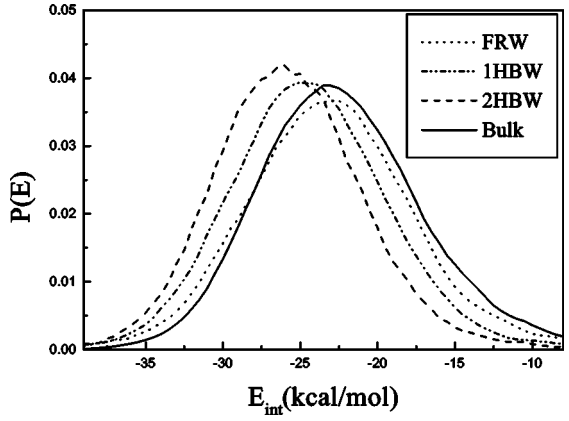


FIG. 8. Distribution of monomer energies of water molecules in the layer $R=1-4$ Å: 1HBW (dash-dotted line), 2HBW (dashed line), FRW (dotted line), and for bulk water (solid line) (from the TBLKC trajectory).

the rest of the system has been plotted in the abscissa. The vertical axis shows the probability. The overall stability in terms of potential energy follow the order FRW < 1HBW < 2HBW.

The ratio 1HBW: 2HBW, which has been found as 10:1, gives a measurement of the free energy difference between these two states. This ratio corresponds to a free energy difference of ~1.4 kcal/mol, which has been calculated from the following equation:

$$\Delta G = -RT \ln \frac{n_1}{n_2}, \tag{10}$$

where the ratios $n_1$ and $n_2$ are the number of two different species which are in equilibrium at temperature $T$ (300 K). The ratio $n_1/n_2$ has been averaged over time. The MHG is actually a $SO_4^-$ group and contains more than one acceptor oxygen atom. So there could have been a formation of two H bonds at a time between a SDS monomer and a water monomer. But in fact it has been observed that the O-O distance (2.3–2.5 Å) in the single MHG does not allow this phenomenon. So 2HBW species always forms double bonds with two different SDS monomers. It is clear that although the second H bond between water monomer and micelle gives some additional stability, the 2HBW is not the most favorable and abundant state.

## IV. DISCUSSION

We have reported here the structure and dynamics of the water around SDS micelle and the energetics controlling these properties. The water monomers present in the first layer of hydration have been found to exist as "bound" or "free." The bound water has further been classified according to its number of H bonds with the MHGO. The dynamics of various types of water species have separately been quantified which give more clear insight than a previous study [23] into the understanding of the "slow water dynamics" at the first layer of hydration around SDS micelles. The rotational dynamics have been separated from translational dynamics during analysis. The calculation of the time constants for the rotational relaxations [Eq. (2)] of the bound water are 0.84 and 2.20 ps (Table II) whereas for the "bulk" water the values obtained from the trajectory TBLKC are 0.37 and 1.67 ps, which is almost the same for the layer $R=9-12$ Å obtained from the trajectory TRAJ1 (0.37 and 1.62 ps). The shorter and longer components for the relaxation become 2.3 and 1.4 times, respectively, for the bound water than the bulk water. The relaxation time for the FRW falls midway between the slowest decay of the bound water and the "fastest" decay of the water at larger (i.e., beyond the first layer) distances. This implies that though FRW is not directly H boned to the MHG, the interaction with micelle as well as the local environment influences its dynamics. The translational dynamics have been studied by calculating the self-diffusion coefficient of water and residence time analysis. The diffusion coefficients values seem to be more realistic for the TIP3P water model used when the system was simulated with a spherical cutoff method coupled with a shifted function. The calculated $D$ values for the run with the PME method have been shown in Table I to be $3.8\times10^{-5}$ cm$^2$/sec for the bulk water which is far from the range of the experimental data [36], whereas using a 12-Å cutoff and shifted potentials we got a value $2.8\times10^{-5}$ cm$^2$/sec, which is much closer to the experiments ($2.3\times10^{-5}$ cm$^2$/sec) [36]. With the PME method the $D$ values obtained for the $R=1-4$ Å and $R=9-12$ Å layers are $3.0\times10^{-5}$cm$^2$/sec and $3.7\times10^{-5}$ cm$^2$/sec respectively, whereas with our simulation technique $D$ values for these two layers were $1.7\times10^{-5}$ cm$^2$/sec and $2.6\times10^{-5}$ cm$^2$/sec, respectively (Table I). This clearly shows that the differences in the mobilities of these two layers are more prominent with the cutoff method. The results for both methods indicate that the layer $R=9-12$ Å has bulk character. Comparing the experimental $D$ values for water at various temperatures (Table I) the low-temperature behavior of the first-layer hydration water becomes very clear. This might arise due to the anomalous vibrational properties of hydration water as suggested in some previous studies [21,28]. Our preliminary calculations indicated a high density of vibrational states in the low-frequency range of the vibrational spectrum of water in accordance with some previous reports for water around micelles [21] and proteins [28]. An in-depth analysis of the vibrational behavior of solvent molecules for the present system will be taken up in the future.

The residence time was analyzed with the measurement of the decay constants of the survival-time correlation function. For bound water the decay constants are 0.5, 3.74, and 27.4 ps, but the contribution from the $\tau_1=0.5$ ps is very small (2%) whereas the $\tau_2=3.74$ ps and $\tau_3=27.4$ ps contribute 59% and 39%, respectively, which clearly indicates that majority of bound water have a large residence time. FRW have a longer component ($\tau_3=22.68$ ps), which is less than that for the bound and its contribution is low (18%). The other two components are also faster than the bound water. The longest component for the FRW ($\tau_3=22.68$ ps) is arising due to the influence of the local environment. It is interesting to note that the fastest component corresponding to $\tau_1=0.41$ ps contributes 60% for the FRW, which is much higher than that for the bound water. The decay constants for the $R=5-8$ Å and $R=9-12$ Å are drastically different than bound or FRW. The very slow component (~22–27 ps) observed at the first hydration layer vanishes in the subsequent layers and the slowest component for $R=9-12$ Å has been found to be 3.46 ps, comparable with the faster components of the bound water. To monitor the existence of a particular H bond the lifetime analysis is more informative than the residence time analysis. It is established from the data that the 1HBW is dynamically much more stable than 2HBW or FRW. The $\tau_3$ for FRW (17.8 ps) is slightly greater than that for 2HBW ($\tau_3=13.6$ ps) but the contribution for FRW is less (30%) than that for 2HBW (39%). The $\tau_2$ for FRW (1.4 ps) is almost 0.6 times of the $\tau_2$ for 2HBW (2.26 ps). The lifetime of FRW also depends on the choice of the thickness of the hydration layer. The longest decay for the 1HBW ($\tau_3=79$ ps) was not observed from the residence time analysis since the residence time for the bound water was averaged over 1HBW and 2HBW.

To understand the involved thermodynamics we have calculated the probability distributions of water-MHG (Fig. 6) and water-water (Fig. 7) interaction energy. The position of the peaks for different species in Figs. 6 and 7 reveal that the MHG-water hydrogen bond is stronger than the water-water hydrogen bond by an amount $\sim 7$ kcal/mol. Due to this reason, the water monomers prefer to form a H bond with MHGO. Figure 8, which is a probability distribution of the water monomer energy of the interaction with the rest of the system, clearly tells us that stability increases in the order FRW $<$ 1HBW $<$ 2HBW. A greater stability of the MHGO-water H bond forces a water monomer to leave the solvent cage formed by other water molecules. The spacing between the peak positions for 1HBW, 2HBW, and FRW indicates that the there is a benefit of $\sim 1.5-2.0$ kcal/mol from each H-bond formation between water and MHGO. The nearly same peak position for the FRW and bulk are indicative of the comparable stability of both species. A similar observation was also reported for the CsPFO system, where the slow dynamics of the bound water was attributed to the strength of the MHGO-water hydrogen bond [19–22]. It has been observed that the 2HBW is not the thermodynamically most favored state at though it has the less potential energy than 1HBW or FRW. This is due to the fact that the 2HBW species is restricted in motion, which causes a loss in entropy and reduces the number of 2HBW species formation. The MHGO-MHGO distance can also be a reason for the poor abundance of 2HBW. If the distance between the two head groups of the micelle is too large, then one water monomer will not be able to form two H bonds with the different head groups simultaneously. Surprisingly the calculation showed that 80% of the O-O distance pairs of SDS micelle could allow the accommodation of at least one 2HBW species. This calculation leads us to the conclusion that it is the loss of freedom for 2HBW species rather than the availability of two "O" acceptors at a chosen geometry that is the main cause of its poor abundance.

The ratio of the number of free and bound water molecules is misleading to calculate the free energy differences between these two states since the number of free water molecules will increase if the thickness of the first layer is increased. In a previous report [23] on the SDS miceller system the FRW: 1HBW: 2HBW has been found to be 33:60:7—i.e., 4.71:8.6:1.0. The number of free water molecules will increase if we take the first hydration layer as $R = 1-5$ Å rather than using $R = 1-4$ Å but the number of 1HBW or 2HBW species will not change since $R = 1-4$ Å already includes all bound water molecules in the system. But it should be reported here that for $R = 1-4$ Å we have observed the ratio 10:10:1.

The effect of the shape and size of the micelle can play an important role in controlling the properties of the hydration water. The works reported in Refs. [19–22] deal with an oblate-shaped micelle and the dimension of micelle is also different from our spherical SDS micelle. For that CsPFO micelle [19–21] the number of donor or acceptor atoms on the polar (carboxylate) head group on each monomer is also less. In spite of these dissimilarities the agreements of the observed properties tell that the shape and size of the micelle has a less effect on the properties we have studied.

## V. CONCLUSIONS

Our investigation includes both structural and dynamical property analysis of water in the first layer of hydration. The structural part includes definitions of the first layer of hydration from radial distribution plots followed by a classification of the water monomer present in the first layer according to its binding and interaction energies with micelle head groups. We have observed three different types of water monomers that have been labeled as FRW, 1HBW, and 2HBW and they have zero, one, and two H bonds with miceller head-group oxygen atoms. The dynamics of these water species have been quantified individually and which give clearer picture than a previous study [23] about the water dynamics around SDS micelle. The residence time of the water and the lifetime of the different water species around SDS micelle presented here were not reported in any article before. The method of simulation adjusted to prevent the overestimation of the diffusion properties of water compared to the experiment. The overestimation of the self-diffusion coefficient of water with the PME technique was observed also for our system which was in agreement with some previous observations [30,37] and that is why we adapted a simulation scheme which would be compatible with the solvent model [37]. The self-diffusion coefficients of the water around SDS micelle reported previously [23] were far away from the range of experimental data and it was indicative of an overestimation of the property which might have been reflected in the other dynamical properties also.

The reason for the slow dynamics in the first hydration layer which has been observed here is due to the fact that the water molecules try to achieve a more stable state by forming a H bond with MHG and become frozen or less mobile compared to that of bulk water. This happens due to the fact that the micelle-water H bond is more stable by an amount $\sim 7$ kcal/mol over the water-water H bond. This fact also creates a concourse of the water molecules at a distance of $\sim 2.7$ Å from the MHGO which has been established from the radial distribution plot. Bound water—i.e., water monomers H bonded to the micelle—is practically frozen both rotationally and translationally compared to the bulk. The FRW and bulk water monomers also form H bonds with other water monomers, and in that sense they are also not free water. We presented here the rotational relaxation and translation dynamics of bound and free water separately and indicated the relative contributions of fast and slow dynamics. An in-depth study shows that the lifetime of the 1HBW species is much longer than the 2HBW or FRW. Since in the Fig. 8 the probability distribution showed that the 2HBW gets maximum stability, it was expected to have highest relative abundance among the three types of species and it should have been also dynamically the most stable. But entropy plays a role here, and to prevent the loss in freedom, the 2HBW species are formed fewer in numbers compared to the 1HBW. Thermodynamically 1HBW is more stable than 2HBW by an amount $\sim 1.4$ kcal/mol which is quite similar to the value observed for the CsPFO system [22]. The ratio FRW:1HBW has been found to be 1:1 although FRW is energetically less stable and the lifetime of the FRW species is

also less compared to 1HBW. This can be interpreted as that our definition of the first layer included a huge number of free water and that is why our observed ratio FRW:1HBW is much different from previous reports on the SDS miceller system and for the CsPFO system [22,23]. Similarities of the data obtained for SDS and CsPFO system strongly suggest that the observed anomalous behavior of water molecules near a micellar surface can be a general feature.

## ACKNOWLEDGMENT

S.G.D. is thankful to CSIR, India, for financial support.

[1] S. K. Pal, J. Peon, B. Bagchi, and A. H. Zewail, J. Phys. Chem. B **106**, 12 376 (2002).
[2] A. R. Bizzarri and S. Cannistraro, J. Phys. Chem. B **106**, 6617 (2002).
[3] S. K. Pal, J. Peon, and A. H. Zewail, Proc. Natl. Acad. Sci. U.S.A. **99**, 1763 (2002).
[4] N. Sarkar, A. Datta, S. Das, and K. Bhattacharyya, J. Phys. Chem. **100**, 15 483 (1996).
[5] A. Datta, D. Mondal, S. K. Pal, and K. Bhattacharyya, J. Mol. Liq. **77**, 121 (1998).
[6] K. Bhattacharyya, Acc. Chem. Res. **36**, 95 (2003).
[7] K. Bhattacharyya and B. Bagchi, J. Phys. Chem. A **104**, 10 603 (2000).
[8] D. Mandal, S. Sen, D. Sukul, and K. Bhattacharyya, J. Phys. Chem. B **106**, 10 741 (2002).
[9] P. Sen, S. Mukherjee, P. Dutta, A. Haldar, D. Mandal, R. Banerjee, S. Roy, and K. Bhattacharyya, J. Phys. Chem. B **107**, 36 277 (2003).
[10] S. G. Dastidar and C. Mukhopadhyay, Phys. Rev. E **68**, 021921 (2003).
[11] V. Makarov, B. M. Pettitt, and M. Feig, Acc. Chem. Res. **35**, 376 (2002).
[12] C. F. Lopez, S. O. Nielsen, K. L. Klein, and P. B. Moore, J. Phys. Chem. B **108**, 6603 (2004).
[13] M. F. Colombo, D. C. Rau, and V. A. Parsegian, Science **256**, 655 (1992).
[14] V. Launnas and B. M. Pettit, Proteins: Struct., Funct., Genet. **18**, 148 (1994).
[15] C. J. Camacho, Z. Weng, S. Vajda, and C. Delisi, Biophys. J. **76**, 1166 (1999).
[16] P. L. Poole and J. L. Finley, Biopolymers **22**, 255 (1983).
[17] C. Chatterjee, B. Majumdar, and C. Mukhopadhyay, J. Phys. Chem. B **108**, 7430 (2004).
[18] C. Chatterjee and C. Mukhopadhyay, Biopolymers **70**, 512 (2003).
[19] S. Pal, S. Balasubramanian, and B. Bagchi, J. Chem. Phys. **82**, 845 (2002).
[20] S. Balasubramanian, S. Pal, and B. Bagchi, Phys. Rev. Lett. **89**, 115505 (2002).
[21] S. Pal, S. Balasubramanian, and B. Bagchi, Phys. Rev. E **67**, 061502 (2003).
[22] S. Pal, S. Balasubramanian, and B. Bagchi, J. Phys. Chem. B **107**, 5194 (2003).
[23] C. D. Bruce, S. Senapati, M. L. Berkowitz, L. Perera, and M. D. E. Forbes, J. Phys. Chem. B **106**, 10 902 (2002).
[24] S. Woutersen, U. Emmerichs, H. K. Nienhuys, and H. J. Bakker, Phys. Rev. Lett. **81**, 1106 (1998).
[25] B. Jonsson, B. Lindman, K. Holmberg, and B. Kronberg, *Surfactants and Polymers in Aqueous Solution* (Wiley, West Sussex, 1998).
[26] J. M. Chen, T. M. Su, and C. Y. Mou, J. Phys. Chem. **90**, 2418 (1986).
[27] A. MacKerell, J. Phys. Chem. **99**, 1846 (1995).
[28] C. Rocchi, A. R. Bizzarri, and S. Cannistraro, Phys. Rev. E **57**, 3315 (1998).
[29] S. E. Feller, R. W. Pastor, A. Rojnucharin, S. Bobusz, and B. R. Brooks, J. Phys. Chem. **100**, 17 011 (1996).
[30] V. A. Makarov, M. Feig, B. K. Andrews, and B. M. Pettitt, Biophys. J. **75**, 150 (1998).
[31] P. Mark and L. Nilsson, J. Phys. Chem. A **105**, 9954 (2001).
[32] V. D. Spoel, P. J. van Maaren, and H. J. C. Berendsen, J. Chem. Phys. **108**, 10 220 (1998).
[33] K. Tasaki, S. McDonald, and J. W. Brady, J. Comput. Chem. **14**, 278 (1993).
[34] Q. Liu, R. K. Schmidt, B. Teo, P. A. Karplus, and J. W. Brady, J. Am. Chem. Soc. **119**, 7851 (1997).
[35] P. E. Smith, H. D. Blatt, and B. M. Pettitt, J. Phys. Chem. B **101**, 3886 (1997).
[36] R. J. Mills, J. Phys. Chem. **77**, 685 (1973).
[37] H. E. Alper, D. Bassolino, and T. R. Stouch, J. Chem. Phys. **98**, 9798 (1993).
[38] H. D. Loof, L. Nilsson, and R. Rigler, J. Am. Chem. Soc. **114**, 4028 (1992).
[39] D. A. McQuarrie, *StatMech* (Harper and Row, New York, 1976).
[40] J. Klafter, G. Zumofen, and A. Blumen, Chem. Phys. **177**, 821 (1993).
[41] D. A. Zichi and P. J. Rosky, J. Chem. Phys. **84**, 2814 (1986).
[42] G. Williams and D. C. Watts, Trans. Faraday Soc. **66**, 80 (1970).
[43] R. Kohlrausch, Ann. Phys. (Leipzig) **12**, 353 (1947).
[44] M. P. Allen and D. J. Tildesley, *Computer Simulation of Molecular Liquids* (Clarendon Press, Oxford, 1987).
[45] R. Chitra and S. Yashonath, J. Phys. Chem. B **101**, 5437 (1997).
[46] A. R. Bizzarri and S. Cannistraro, Phys. Rev. E **53**, R3040 (1996).